

# Nuclei, Superheavy Nuclei and Hypermatter in a chiral $SU(3)$ -Model

Ch. Beckmann \*, P. Papazoglou, D. Zschesche

S. Schramm, H. Stöcker, W. Greiner

*Institut für Theoretische Physik*

*Johann Wolfgang Goethe Universität, D-60054 Frankfurt am Main*

arXiv:nucl-th/0106014v1 6 Jun 2001

---

\*Christian Beckmann, Institut für Theoretische Physik, Universität Frankfurt am Main, Robert-Mayer-Str. 8-10, 60325 Frankfurt am Main, Germany, Tel.:+49-(0)69-7982-2630, Fax:-8350, e-Mail: beckmann@th.physik.uni-frankfurt.de

A model based on chiral  $SU(3)$ -symmetry in nonlinear realisation is used for the investigation of nuclei, superheavy nuclei, hypernuclei and multistrange nuclear objects (so called MEMOs). The model works very well in the case of nuclei and hypernuclei with one  $\Lambda$ -particle and rules out MEMOs. Basic observables which are known for nuclei and hypernuclei are reproduced satisfactorily. The model predicts  $Z=120$  and  $N=172, 184$  and  $198$  as the next shell closures in the region of superheavy nuclei. The calculations have been performed in self-consistent relativistic mean field approximation assuming spherical symmetry. The parameters were adapted to known nuclei.

## A. Introduction

The theory of strong interactions (QCD) is currently still unsolvable in the nonperturbative low-energy regime. Therefore different approaches have to be found for predicting nuclear properties. A promising ansatz are the effective hadronic field theories. Extensive studies of nuclei and hypernuclei have been done in this field. The probably most common effective models are relativistic mean field models [44]. Important work has been done for example by S. wiok et al. [15] as well as K. Rutz, J. Maruhn, P.-G. Reinhard et al. (e.g. [38]). Also hypermatter has been investigated up to extreme objects with various combinations of hyperons (e.g. [29,21,27,36,39–42]).

In the present work we expand this ansatz. Here we develop a model closer to the symmetry of the elementary theory, i.e. QCD. Therefore we construct a Lagrange density, which is largely chiral symmetric, similar to the linear sigma-model [26]. The chiral symmetry is indeed broken explicitly to give the pseudoscalar mesons, the goldstone bosons, a mass and to model the larger finite mass of the strange quark in the hyperon sector.

The model has already been applied successfully to infinite nuclear matter [23].

The present paper presents the investigations of finite nuclei, superheavy nuclei and hypernuclei with one and more hyperons in this framework.

## B. The model

For our investigations we introduce an effective model based on chiral symmetry in nonlinear realisation. The nonlinear realisation of chiral symmetry has been chosen because in the linear version [24] the coupling of the spin-0-mesons to the baryons is restricted to the symmetric coupling (d-type), while in accordance with the vector-meson-dominance the vector mesons couple antisymmetrically to the baryons. The result is a disturbance of the balance between the repulsion of the vector field and the attraction of the scalar field in the nucleonic potential. There is a natural coupling of the nucleon to the strange scalar ( $\zeta$ ) field but not to the corresponding strange vector field  $\phi$ . As a result the scalar attraction is not compensated by an adequate vector repulsion.

We will now discuss our specific Lagrangian. For our calculations we worked in the mean-field-approximation, that means quantum fluctuations of the meson fields are neglected and the quantum fields are replaced by their expectation values:

$$\begin{aligned}\omega &= \langle \omega_0 \rangle \\ \rho &= \langle \rho_0 \rangle\end{aligned}\tag{1}$$

In case of the vector mesons ( $\rho$ ,  $\omega$ ,  $\phi$ ), the space like parts vanish due to isotropy and only the time component survives. The pion-expectation value vanishes because of good parity in the groundstate. Furthermore we adopt the no-sea-approximation and perform all calculations in spherical symmetry.

Finally we get the following Lagrangian:

$$\begin{aligned}\mathcal{L}_{\text{kin}} &= i \sum_i \bar{B}_i \gamma_i \partial^\mu B_i - \frac{1}{2} \sum_{\Phi=\sigma,\zeta,\chi,\omega,\phi,\rho,A} \partial_\mu \Phi \partial^\mu \Phi \\ \mathcal{L}_{\text{int}} &= - \sum_i \bar{B}_i \gamma_0 \left[ g_{i\omega} \omega_0 + g_{i\rho} \tau_3 \rho_0 + g_{i\phi} \phi_0 + \frac{1}{2} e(1 + \tau_3) A_0 + m_i^* \gamma_0 \right] B_i \\ \mathcal{L}_{\text{vec}} &= - \frac{1}{2} k_0 \frac{\chi^2}{\chi_0^2} (m_\omega^2 \omega^2 + m_\rho^2 \rho^2) + g_4^4 (\omega^4 + 6\omega^2 \rho^2 + \rho^4) \\ \mathcal{L}_0^{\text{chi}} &= - \frac{1}{2} k_0 \chi^2 (\sigma^2 + \zeta^2) + k_1 (\sigma^2 + \zeta^2)^2 + k_2 \left( \frac{\sigma^4}{2} + \zeta^4 \right)\end{aligned}$$

$$\begin{aligned}
& +k_3\chi\sigma^2\zeta + k_{3m}\chi\left(\frac{\sigma^3}{\sqrt{2}} + \zeta^3\right) - k_4\chi^4 \\
& -\frac{1}{4}\chi^4\ln\frac{\chi^4}{\chi_0^4} + \frac{\delta}{3}\chi^4\ln\frac{\sigma^2\zeta}{\sigma_0^2\zeta_0} \\
\mathcal{L}_{\text{SB}} = & -\left(\frac{\chi}{\chi_0}\right)^2 [x\sigma + y\zeta]
\end{aligned} \tag{2}$$

with  $x = m_\pi^2 f_\pi$  and  $y = \sqrt{2}m_K^2 f_K - \frac{1}{\sqrt{2}}m_\pi^2 f_\pi$ . The fields  $B_i$  represent the baryons considered, i.e. nucleons in the case of normal nuclei and furthermore hyperons for the investigation of hypernuclei.

The incorporated mesons are the scalar non-strange ( $\sigma$ ) and strange ( $\zeta$ ) mesons, the vector mesons  $\omega$ ,  $\phi$  and  $\rho$  and the coulomb-field  $A$ . Furthermore a scalar glueball field  $\chi$  has been taken into account for the broken scale invariance [23]. The second part of the Lagrangian exhibits the interaction between baryons and mesons and the photon. Here  $m_i^*$  is the effective mass of the baryon species  $i$  which is generated by the interaction with the scalar mesons:

$$m_i^* = g_{i\sigma}\sigma + g_{i\zeta}\zeta \quad . \tag{3}$$

The asterisk indicates that the masses in the medium shift with the changing scalar fields  $\sigma$  and  $\zeta$ . The third part  $\mathcal{L}_{\text{vec}}$  contains the vector meson mass terms as well as a quartic vector meson self interaction. The term  $\mathcal{L}_0$  indicates the potential of the scalar fields of the model. The logarithmic terms in the potential break the scale invariance [23]. The spontaneously broken symmetry leads to the existence of massless Goldstone modes which are eliminated from the theory by the last term of the Lagrangian, which explicitly breaks the chiral symmetry.

For the finite-nucleus calculation we also considered pairing effects in a simple approximation. The pairing was parametrized in an isospin symmetric way with the *Constant-Gap-Model* [7].

### C. Adjustment of the Parameters

The free parameters of the model have been adjusted to the properties of finite nuclei in a least square fit. The function to minimize is defined as

$$\chi^2 = \sum_n \left( \frac{O_n^{\text{exp}} - O_n^{\text{theo}}}{\Delta O_n} \right)^2 \quad , \tag{4}$$

where  $O^{\text{exp}}$  are the experimental and  $O^{\text{theo}}$  the calculated values of the observables. The value  $\Delta O$  is used to weight the different observables.

The following nuclei enter into the fit:

$$^{16}\text{O}, ^{40}\text{Ca}, ^{48}\text{Ca}, ^{58}\text{Ni}, ^{90}\text{Zr}, ^{112}\text{Sn}, ^{124}\text{Sn}, ^{208}\text{Pb} \quad . \tag{5}$$

These nuclei are spherical and the excited states are not too close to the ground state, so their influence is minimal. The observables that are relevant for the fit are the binding energy  $E_B$ , the charge diffraction radius  $R_{\text{diff}}$ , the surface thickness  $\sigma_O$  and in some cases the binding energy of  $^{264}\text{Hs}$ , as discussed below. The values of the observables used for the fit have been taken from [25], the minimization procedure used is Powell's method [31].

### D. The Parameters

The parameters, varied in the  $\chi^2$ -fit, are the coupling constant between the nucleons and the  $\omega$ -meson  $g_{N\omega}$ , the coupling constant between the nucleons and the  $\rho$ -meson  $g_{N\rho}$ , which primarily determines the isospin dependent part of the nuclear force, the vacuum expectation value of the gluon condensate  $\chi_0$ , the decay constant of the kaon  $f_K$ , the coupling constant of the quartic self interaction of the  $\omega$ -vector meson  $g_4$ , and the parameters of the potential of the scalar mesons  $k_1$  and  $k_2$ . The absolute values of the parameters and their change in the fit are shown in Table I. For the set  $C_1$  the parameters were adjusted to the vacuum properties of the mesons as well as to the properties of infinite nuclear matter [23]. The set  $C_1^{\text{nuc}}$  has been derived from a fit to finite nuclei as outlined above. We have also performed a fit suitable for extrapolating superheavy nuclei, which includes the binding energy of  $^{264}\text{Hs}$  but disregards the observables of  $^{16}\text{O}$ . The resulting parameter set is called  $C_1^{\text{hs}}$ .

To understand the significance of the variations in the parameters, we consider the sensitivity of  $\chi^2$  with respect to the parameters. One finds that  $\chi^2$  is very sensitive to the value of  $g_{N\omega}$ : a change of  $g_{N\omega}$  of 0.25 % leads to a variation of  $\chi^2$  of about 85 %. Varying the gluon field  $\chi_0$  by 2% would even result in a change of  $\chi^2$  by many orders of magnitude. The like is true for  $g_4$ ,  $k_1$  and  $k_3$ . In contrast  $f_K$ , entering the symmetry breaking part of the Lagrangian, Eq.2, does not change considerably. In general we see that the parameters change appreciably due to the fit.

## E. Known Nuclei

### 1. The Change of the Fit-Observables

Table II shows the absolute and relative change of the parameters entering the fit, due to the adaption of the parameters. The fit improves the results by more than a factor of 20. For all nuclei the binding energy has changed most compared to the original nuclear matter fit  $C_1$ . The diffraction radius changes little, for lead there is even a slightly worse result than in the fit to infinite nuclear matter.

### 2. The Formfactor

We now want to employ our model to finite nuclei with known properties. Their observables enter into the adjustment of the parameters. Figures 1, 2 and 3 show the charge form factors of oxygen, calcium and lead. The experimental values have been taken from [43]. Here the position of the first null and the first maximum are of particular interest, because they determine the charge diffraction radius and the surface thickness. We find that both parameter sets lead to very similar results, but all calculations show moderate deviations from the experiment [43]. The first null in the formfactor of oxygen lies at about 2 % higher momentum as in the experiment. This leads to a slightly smaller nucleus. Moreover, the surface of the nucleus is too thin, as visible in the deviation of about 7 % at the first maximum. Calcium agrees significantly better with the experiment. For lead the first null is at slightly ( $\sim 1\%$ ) too small momenta, which results in a nucleus which is somewhat too big.

### 3. The Single Particle Energies for Neutrons

Figure 4 shows the single-particle energies for neutrons in  $^{208}\text{Pb}$  (The experimental values are taken from [11]). We find a good reproduction of the spin-orbit splitting while the absolute positions of the energy-levels deviate significantly from the experimental values. Adapting the parameters to finite nuclei ( $C_1^{\text{nuc}}$ ) results in a shift of the energy-levels, which is obvious because the total binding energy enters into the fit and experiences a noticeable change (See Table II). It is remarkable that the relative distances between the levels are scarcely changed. The single particle energies are mostly shifted together. Furthermore it was not possible to find a set of parameters with a different distribution of the energy levels, even by changing single parameters by hand.

### 4. Shell Closures and Magic Nuclei

The model reproduces all known magic numbers correctly. Exemplarily Fig. 5 shows the two-nucleon gap energy

$$\delta_{2n}(Z, N) = S_{2n}(Z, N) - S_{2n}(Z, N + 2) \quad (6)$$

$$\delta_{2p}(Z, N) = S_{2p}(Z, N) - S_{2p}(Z + 2, N) \quad (7)$$

with the two-nucleon separation energy

$$S_{2n}(Z, N) = E_B(Z, N - 2) - E_B(Z, N) \quad (8)$$

$$S_{2p}(Z, N) = E_B(Z - 2, N) - E_B(Z, N) \quad (9)$$

The binding energy is given by

$$E_B = E_{\text{total}} - Am_N \quad . \quad (10)$$

The peaks indicate the magic numbers, in this case  $Z = 82$  for protons and  $N = 126$  for neutrons. Fitting the model parameters to finite nuclei instead of infinite nuclear matter does not change the magic numbers. This also holds for all other known magic nuclei. It should be noticed that of course the binding energies per nucleon do change with the fit.

## F. Superheavy Nuclei

The investigation of nuclei with more than 100 protons has recently received renewed interest. After the elements 110 and 112 [19,20], produced at GSI in Darmstadt, remained the heaviest isotopes for several years, it was possible to produce nuclei with 114 and 116 protons at Dubna in 1999 [33], a nucleus with 118 protons might have been observed in a Berkeley experiment [30]. The quest for superheavy nuclei is motivated by the prediction of shell closures beyond  $Z=110$ . In the past such calculations have already been done in relativistic mean field models, for example [38,3] predicting  $Z=114$  and  $Z=120$  and [15] predicting  $Z=126$ . In the following we want to present the results of the chiral model developed here.

### 1. Shell Closures

The chiral model predicts clearly  $Z=120$  as the next shell closure, while another one at  $Z=114$  is visible but weak. Fig. 6 shows the binding energy, the two nucleon separation energy and the two-nucleon gap for nuclei with 184 neutrons and varying proton numbers (left side) and for nuclei with 120 protons and varying neutron numbers (right side). The parameter sets used here are explained above. The major change happens with the use of parameters fitted to finite nuclei instead of infinite nuclear matter. The most important point to mention here is the suppression of the peak in the two-proton gap at the proton number of  $Z=114$ . We find that it is clearly smaller in the calculation with  $C_1^{\text{nuc}}$  compared to  $C_1$  and it is even more suppressed when using the set  $C_1^{\text{hs}}$ .

In conclusion we find that  $Z=114$  is at best a subshell closure in this chiral model, while  $Z=120$  is probably the next shell closure which shows a distinctly pronounced peak. Furthermore it should be mentioned that this nucleus is still above the drip line which shifts to higher  $Z$  in the fit to nuclei compared to the nuclear matter fit. For neutrons we find the next magic numbers at  $N=172$ ,  $N=184$  and  $N=198$ .

### 2. Charge Distribution and $\alpha$ - Decay

A specialty of superheavy nuclei seems to be their charge distribution which is shown in Fig. 7 for the model in question. One finds a noticeable decrease of the charge density in the center of the nucleus. This observation has also been made in calculations in the Walecka model [3]. Could this behaviour be the result of a structure of the nucleus, which reminds of the bucky balls in organic chemistry ? The nucleus in question has 120 protons what corresponds to 60  $\alpha$ -particles. These could form a bucky ball structure hold together by valence neutrons. Lighter objects of this type have been investigated earlier by W. von Oertzen [32].

The characteristic observables for the identification of superheavy nuclei are the energies of the  $\alpha$ -particles emitted during the decay. The resulting energies in the chiral model are shown in Fig. 8. One finds that these energies are almost constant in the region from  $Z=118$  to  $Z=108$ . This is in *qualitative* agreement with the possible findings of the Berkeley group which found the nucleus  $^{293}118_{175}$ . At this point one should keep in mind of course that our calculations are all done in spherical approximation.

## G. Hypernuclei

We now want to apply the chiral model to nuclei including hyperons. Hypernuclei have been first observed by Danysz and Paiewski in 1953 [16]. Hypernuclei have a lifetime of about  $10^{-10}$ s which makes it particularly difficult to investigate heavy ones. In the seventies, hypernuclei with up to  $A=15$  have been produced [12] and some years later even heavier hypernuclei could be observed at CERN [9,10,4-6] and AGS [8,13,28,14] where also excited states have been investigated.

A theoretical description of hypernuclei was tried among others in Skyrme-Hartree-Fock-models (e.g. [29,21]) and relativistic mean-field models [27,36].

In the following calculations of hypernuclei in the chiral  $SU(3)$ -Model shall be investigated.

Fig. 9 shows the single particle energies of  $\Lambda$ -particles in different nuclei (Experiment: [1,18]). Here the binding energy of  $\Lambda$ -particles is plotted against  $A^{-2/3}$ , i.e. the inverse of the surface of the nucleus. The parameters were adapted to finite nuclei ( $C_1^{\text{nuc}}$ ). All single particle levels meet for  $A \rightarrow \infty$  at the value of the  $\Lambda$ -potential (-28 MeV) in nuclear matter as it should be. However one should keep in mind that it is possible to modify the depth of the hyperon potential in nuclear matter by the explicit symmetry-breaking in strangeness direction without effecting the properties of normal nuclei [23]. One achievement of the model is the correct description of the  $\Lambda$ -levels in finite nuclei, that is the reproduction of the measured single-particle-energies, which is particularly successful for the deeper bound states. An exception is the 1s-niveau in  $^{208}\text{Pb}$  which is deeper bound than in our calculation. However this experimental result also contradicts a nuclear matter potential of -28 MeV, because the  $\Lambda$ -level itself lies at -26.5 MeV and the determination of the nuclear matter potential is done by extrapolating the  $\Lambda$ -levels in finite nuclei. The situation is similar to calculations in relativistic mean-field models [39,37], where one finds even less deeply bound states.

Fig. 10 shows the binding energy of  $\Lambda$ -baryons in light nuclei (It was calculated the 1s-level in a nucleus without  $\Lambda$ ). The experimental data have been taken from [22]. In the region of light nuclei the calculations agree very well with the experiment, for heavier nuclei the divergence gets larger. This is especially astonishing since one would expect larger errors for light nuclei in a mean field calculation. The substantial point is here that the calculations show a different trend than the experiments. Furthermore the energy differences between nuclei of equal masses are not reproduced in the calculations. Anyhow, the result is satisfying since the only hypernucleus observable entering the model, is the nuclear matter potential of the  $\Lambda$ .

Since the model provides reasonable results for nuclei with only one  $\Lambda$ , it is quite interesting to investigate nuclei with more than one  $\Lambda$ . However this field is experimentally largely unexplored. The only nuclei ever observed with more than one  $\Lambda$  are  $^6_{\Lambda\Lambda}\text{He}$ ,  $^{10}_{\Lambda\Lambda}\text{Be}$  and  $^{13}_{\Lambda\Lambda}\text{Be}$  [17,35,2].

Fig. 11 shows the calculated binding energies for  $^{16}\text{O}$  and  $^{40}\text{Ca}$  with a varying number of added  $\Lambda$ -particles. One finds minima at non-zero numbers of added  $\Lambda$  for oxygen and calcium. This is not surprising because with the  $\Lambda$ -particles a new degree of freedom has been opened. The  $\Lambda$ -potential is below the highest occupied nucleonic state.

All shown nuclei are stable, because the target states of the decay are occupied with nucleons (Pauli-Blocking).

The basis for the good description of  $\Lambda$ -hypernuclei is given by the correct value of the  $\Lambda$ -potential in infinite nuclear matter. We will see in the next section that this is not fulfilled for the other hyperons which leads to problems with the investigation of e.g.  $\Xi$ -matter.

## H. MEMOS

While experimental results for nuclei with one hyperon exist for some time, there is almost nothing known about objects with a higher amount of strangeness. We now want to investigate, if nuclear objects containing  $\Xi$ -hyperons (metastable, exotic multistrange objects (MEMOs)) are stable against strong decay in the investigated model. Experimentally no strange objects, additional to those mentioned above, are known.

Theoretically MEMOs were investigated copiously in Walecka-type mean-field-models [39–42]. There in fact the authors find possibilities of combining hyperons, which lead to metastable objects.

In the current chiral model substantial difficulties occur due to the fact that the hyperon potentials are not described correctly.

For the correct description of the  $\Lambda$ -potential in nuclear matter an explicit symmetry breaking term has been included, which does not violate the PCAC-relation [34]:

$$\mathcal{L}_{\text{hyp}} = m_3 \text{Sp} (\overline{B}B + \overline{B}[B, S]) \text{Sp}(X - X_0) \quad (11)$$

with  $S_b^a = -\frac{1}{3}[\sqrt{3}(\lambda_8)_b^a - \delta_b^a]$ . The parameter  $m_3$  is used to fix the  $\Lambda$ -potential at -28 MeV. The other hyperon potentials are determined by this. This leads to a repulsive  $\Xi$ -potential of 30.3 MeV. The potential of  $\Xi$ -particles in  $\Xi$ -matter is about 126 MeV at nuclear density and thus strongly repulsive as shown in Table III. One also finds that the  $\Lambda$ -potential in  $\Lambda$ -matter is repulsive.

In summary there is no combination of  $\Lambda$ - or  $\Xi$ -particles which would lead to bound states. The only stable combinations are given by  $\Lambda$ -particles in nuclear matter as shown in the previous section. Furthermore the model predicts that  $\Xi$ -hypernuclei cannot exist because the nucleon- $\Xi$ -potential is repulsive, too.

If one neglects the explicit symmetry breaking in the strange sector completely the model yields attractive potentials between hyperons (Table IV), but on the other hand the model is not able to reproduce a single hyperon-observable

correctly. For example the potential of  $\Lambda$ -particles in nuclear matter is then  $U_\Lambda=-100$  MeV which is far too deep. The same is true for the  $\Xi$ -potential with  $U_\Xi=-115$  MeV.

Another possibility to make the existence of MEMOs possible is to include a further parameter to the symmetry breaking. In this case it is possible to make the hyperon potentials a bit less repulsive, but nevertheless they stay repulsive, so MEMOs can not exist (Table V). Admittedly nuclei are possible in this case which include nucleons together with  $\Xi$ -hyperons, because their potentials in nuclear matter are attractive. For example a  ${}^4\text{He}$  nucleus with maximum two  $\Xi$ -particles is imaginable, in  ${}^{16}\text{O}$  even four bound  $\Xi$ -states could be possible if one takes into account the change of the potential due to the added hyperons. It should nevertheless be mentioned that all these nuclei would not be stable against strong decay, because the nucleon states, in those the hyperons would decay are not occupied.

## I. Conclusion

A chiral  $SU(3)$ -model has been applied to different forms of finite nuclear matter. The model is based on chiral symmetry in nonlinear realisation. All calculations have been performed in mean-field-approximation and spherical symmetry. The parameters have been fitted to properties of finite nuclei.

The model shows a clear improvement of the results compared to calculations with parameters fitted to infinite nuclear matter. All charge distributions of spherical nuclei can be reproduced satisfactorily. Furthermore all known shell closures are described correctly. The qualitative results are very robust against changes of the parameters.

In the regime of superheavy nuclei the model predicts clearly  $Z=120$  as the next magic number. The closure at  $Z=114$ , which is often shown in non-relativistic models, is not validated by our model. For the neutrons the model yields  $N=172$ ,  $N=184$  and  $N=198$  as magic numbers. These results are widely independent of the parameter set. For  $Z=120$  the charge distribution shows a strong depletion in the center of the nucleus.

Hypernuclei have also been investigated. The potential of the  $\Lambda$ -particles could be fixed by the explicit symmetry breaking term. One then observes a very good reproduction of the experimental data. In particular some nuclei with one or more  $\Lambda$ -particles are resistant against strong decay.

Major problems appear with objects containing  $\Xi$ -hyperons or those that contain no normal nucleons at all (MEMOs). Because all hyperon-hyperon-potentials are repulsive, there is not a single bound hypernucleus built up from hyperons alone. Furthermore the potential of  $\Xi$ -particles in nuclear matter is positive.

## J. Outlook

Up to now all calculations have been performed in spherical symmetry. Specially for superheavy nuclei it is most interesting to investigate the influence of deformation. A further investigation of the density-depletion in the center of  $Z=120$  is desirable, particularly under the aspect of cluster formation. The question about the existence of MEMOs has to be investigated further. The preferable solution would be to find a term which describes all hyperon potentials correctly but does not introduce new parameters which have to be adjusted. Possibly one will have to change the model on more basic level and has to introduce an additional scalar condensate, which is not the chiral partner of the pion. Investigations along this line are in progress.

## K. Acknowledgements

This work was supported by GSI, BMBF, DFG and the Josef Buchmann Stiftung.

- 
- [1] S. Ajimuetra et al., Nucl. Phys. **A585** (1995) 173c
  - [2] S. Aoki et al., Prog. Theor. Phys. **85** (1991) 1287
  - [3] M. Bender, K. Rutz, P.-G. Reinhard, J. A. Maruhn, W. Greiner, Phys. Rev. **C60** 034304 (1999)
  - [4] R. Bertini et al., Phys. Lett. **B83** (1979) 306
  - [5] R. Bertini et al., Phys. Lett. **B90** (1980) 375
  - [6] R. Bertini et al., Nucl. Phys. **A360** (1981) 315

- [7] J. Blocki, H. Flocard, Nucl. Phys. **A273** (1976) 45
- [8] G. C. Bonnazzola, T. Bressani, R. Cester, E. Chiavassa, G. Dellacasa, A. Fainberg, N. Mirfakhrai, A. Musso, G. Rinaudo, Phys. Lett. **B53** (1974) 297
- [9] W. Brückner et al., Phys. Lett. **B62** (1976) 481
- [10] W. Brückner et al., Phys. Lett. **B79** (1978) 157
- [11] X. Campi, D. W. Sprung, Nucl. Phys. **A194** (1972) 401
- [12] T. Cantwell et al., Nucl. Phys. **A236** (1974) 445
- [13] R. E. Chrien et al., Phys. Lett. **B89** (1979) 31
- [14] R. E. Chrien et al., Nucl. Phys. **A478** (1988) 705c
- [15] S. Ćwiok, J. Dobaczewski, P.-H. Heenen, P. Magierski, W. Nazarewicz, Nucl. Phys. **A611** (1996) 211
- [16] M. Danysz, J. Pniewski, Phil. Mag. **44**, (1953) 348
- [17] M. Danysz et al., Phys. Rev. Lett. **11** (1963) 20
- [18] T. Hasegawa et al., Phys. Rev. **C53** (1996) 1210
- [19] S. Hofmann, V. Ninov, F. P. Hessberger, P. Armbruster, H. Folger, G. Münzenberg, H. J. Schött, A. G. Popeko, A. V. Yeremin, A. N. Andreyev, S. Saro, R. Janik, M. Leino, Z. Phys. **A350** (1995) 277 and Z. Phys. **A350** (1995) 281
- [20] S. Hofmann, V. Ninov, F. P. Hessberger, P. Armbruster, H. Folger, G. Münzenberg, H. J. Schött, A. G. Popeko, A. V. Yeremin, S. Saro, R. Janik, M. Leino, Z. Phys. **A354** (1996) 229
- [21] F. Ineichen, D. Von-Eiff, M. K. Weigel, J. Phys. **G**, Nucl. Part. Phys. **22** (1996) 1421
- [22] M. Juric et al., Nucl. Phys. **B52** (1973) 1
- [23] P. Papazoglou, D. Zschesche, S. Schramm, J. Schaffner-Bielich, H. Stöcker, W. Greiner, Phys. Rev. **C59** (1998) 411
- [24] P. Papazoglou, D. Zschesche, S. Schramm, J. Schaffner-Bielich, H. Stöcker, W. Greiner, Phys. Rev. **C55** (1997) 1499
- [25] J. Friedrich, P.-G. Reinhard, Phys. Rev. **C33** (1986) 335
- [26] M. Gell-Mann, M. Levy, Nuovo Cim. **16**, 705 (1960)
- [27] J. Mares, J. Zofka, Z. Phys. **A333** (1989) 209
- [28] M. May et al., Phys. Rev. Lett. **47** (1981) 1106
- [29] D. J. Millner, C. B. Dover, A. Gal, Phys. Rev. **C38** (1988) 2700
- [30] V. Ninov et al., Phys. Rev. Lett. **83** 1104 (1999)
- [31] W. H. Press, B. P. Flannery, S. A. Teukolsky, W. T. Vetterling, "Numerical Recipes", Cambridge University Press, 1996
- [32] W. von Oertzen, Z. Phys. **A354** (1995) 37
- [33] Y. Oganessian et al., Nature (London) **400** (1999) 242
- [34] P. Papazoglou, Dissertation, Universität Frankfurt am Main, 1998
- [35] D. J. Prowse, Phys. Rev. Lett. **17** (1966) 782
- [36] M. Rufa, P.-G. Reinhard, J. A. Maruhn, W. Greiner, M. R. Strayer, Phys. Rev. **C38** (1988) 390
- [37] M. Rufa, J. Schaffner, J. A. Maruhn, H. Stöcker, W. Greiner, P. G. Reinhard, Phys. Rev. **C42** (1990) 2469
- [38] K. Rutz, M. Bender, T. Bürvenich, T. Schilling, P.-G. Reinhard, J. A. Maruhn, W. Greiner, Phys. Rev. **C56** (1997) 238
- [39] J. Schaffner, C. Greiner, H. Stöcker, Phys. Rev. **C46** (1992) 322
- [40] J. Schaffner, C. B. Dover, A. Gal, C. Greiner, H. Stöcker, Phys. Rev. Lett. **71** (1993) 1328
- [41] J. Schaffner, Dissertation, Universität Frankfurt am Main, 1994
- [42] J. Schaffner, C. B. Dover, A. Gal, C. Greiner, D. J. Millener, H. Stöcker, Ann. Phys. **235** (1994) 35
- [43] H. de Vries, C. W. de Jager, C. de Vries, Atomic Data and Nuclear Data Tables **26** (1987) 495
- [44] B. D. Serot, J. D. Walecka, *Advances in Nuclear Physics*, Vol. 16

	$C_1$	$C_1^{\text{nuc}}$	$C_1 - C_1^{\text{nuc}}$	$C_1 - C_1^{\text{nuc}}$ [%]
$g_{N\omega}$	13.6065	13.5723	0.0342	0.25
$\chi_0$	401.93	409.77	-7.84	-1.95
$f_K$	122.0	122.143	-0.143	-0.12
$g_4$	61.47	74.57	-13.1054	-21.32
$k_1$	1.399	1.354	0.0456	3.256
$k_3$	-2.6525	-2.773	0.12	-4.542
$g_{N\rho}$	4.5355	5.6579	-1.1224	-24.75

TABLE I. The parameters used with the model and their change due to the fit to finite nuclei.



	$^{16}\text{O}$			$^{40}\text{Ca}$			$^{208}\text{Pb}$			$\chi^2$
	E/A (MeV)	$R_{\text{diff}}(fm)$	$\sigma_{\text{O}}(fm)$	E/A	$R_{\text{diff}}$	$\sigma_{\text{O}}$	E/A	$R_{\text{diff}}$	$\sigma_{\text{O}}$	
Exp.	-7.98	2.78	0.84	-8.55	3.85	0.98	-7.86	6.81	0.90	
$C_1$	-7.30	2.68	0.79	-8.00	3.80	0.92	-7.56	6.79	0.87	7749
$C_1^{\text{nuc}}$	-7.95	2.7	0.81	-8.62	3.81	0.94	-7.91	6.86	0.89	361

TABLE II. The values of the fit observables for paramters adapted to infinite nuclear matter ( $C_1$ ) as well as finite nuclei ( $C_1^{\text{nuc}}$ ).

	N	$\Lambda$	$\Xi$
N-matter	-71.04	-28.23	+30.27
$\Lambda$ -matter	-38.13	+20.45	+85.78
$\Xi$ -matter	+16.17	+73.83	+126.75

TABLE III. Baryon potentials (in MeV) in different environments including explicit symmetry breaking.

	N	$\Lambda$	$\Xi$
N-matter	-71.04	-100.6	-114.46
$\Lambda$ -matter	-97.31	-89.2	-73.27
$\Xi$ -matter	-126.94	-90.57	-56.59

TABLE IV. Baryon potentials (in MeV) in different environments without explicit symmtry breaking.

	N	$\Lambda$	$\Xi$
N-matter	-71.04	-28.23	-42.09
$\Lambda$ -matter	-38.13	+20.45	+30.68
$\Xi$ -matter	-60.16	+21.06	+49.43

TABLE V. Baryon potentials (in MeV) with a symmetry-breaking, including an additional parameter.

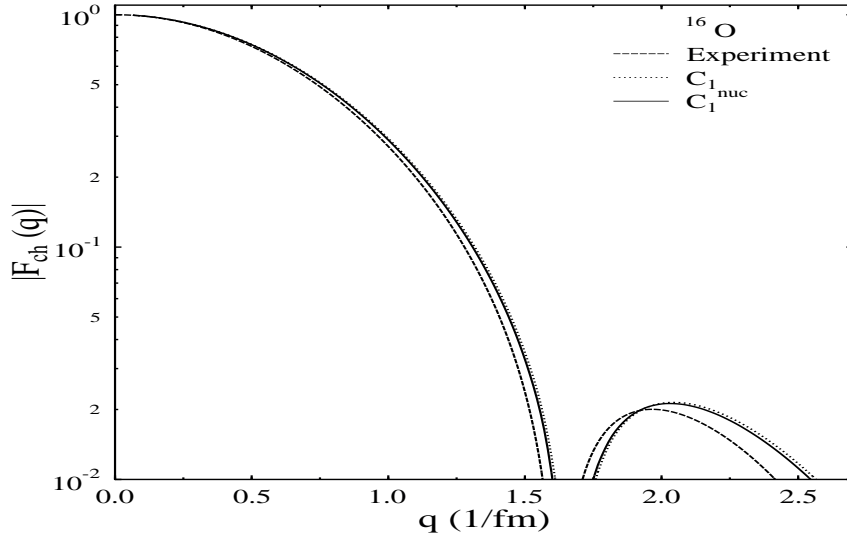


FIG. 1. Charge Form Factor of  $^{16}\text{O}$ .

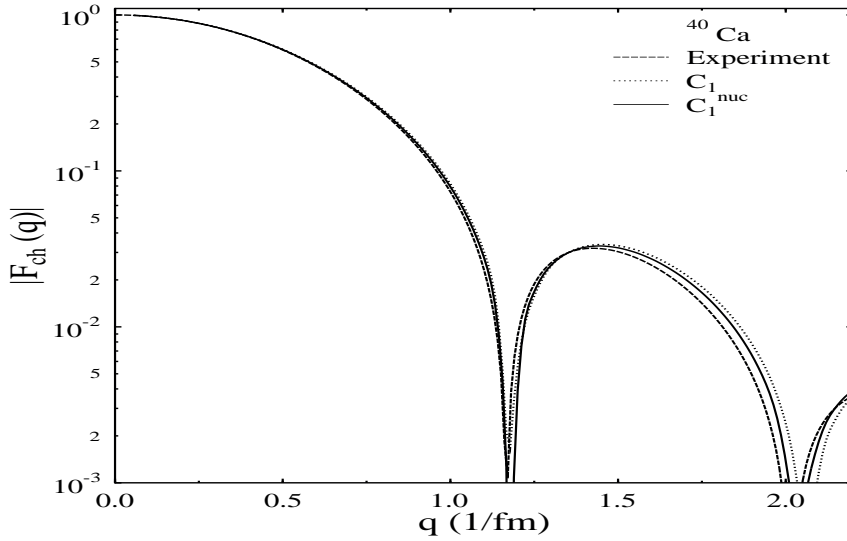


FIG. 2. Charge Form Factor of  $^{40}\text{Ca}$ .

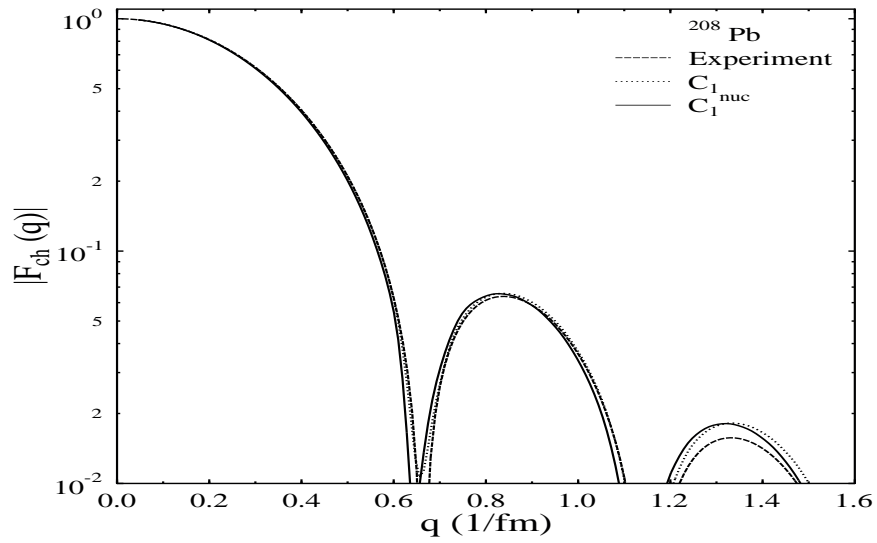


FIG. 3. Charge Form Factor of  $^{208}\text{Pb}$ .

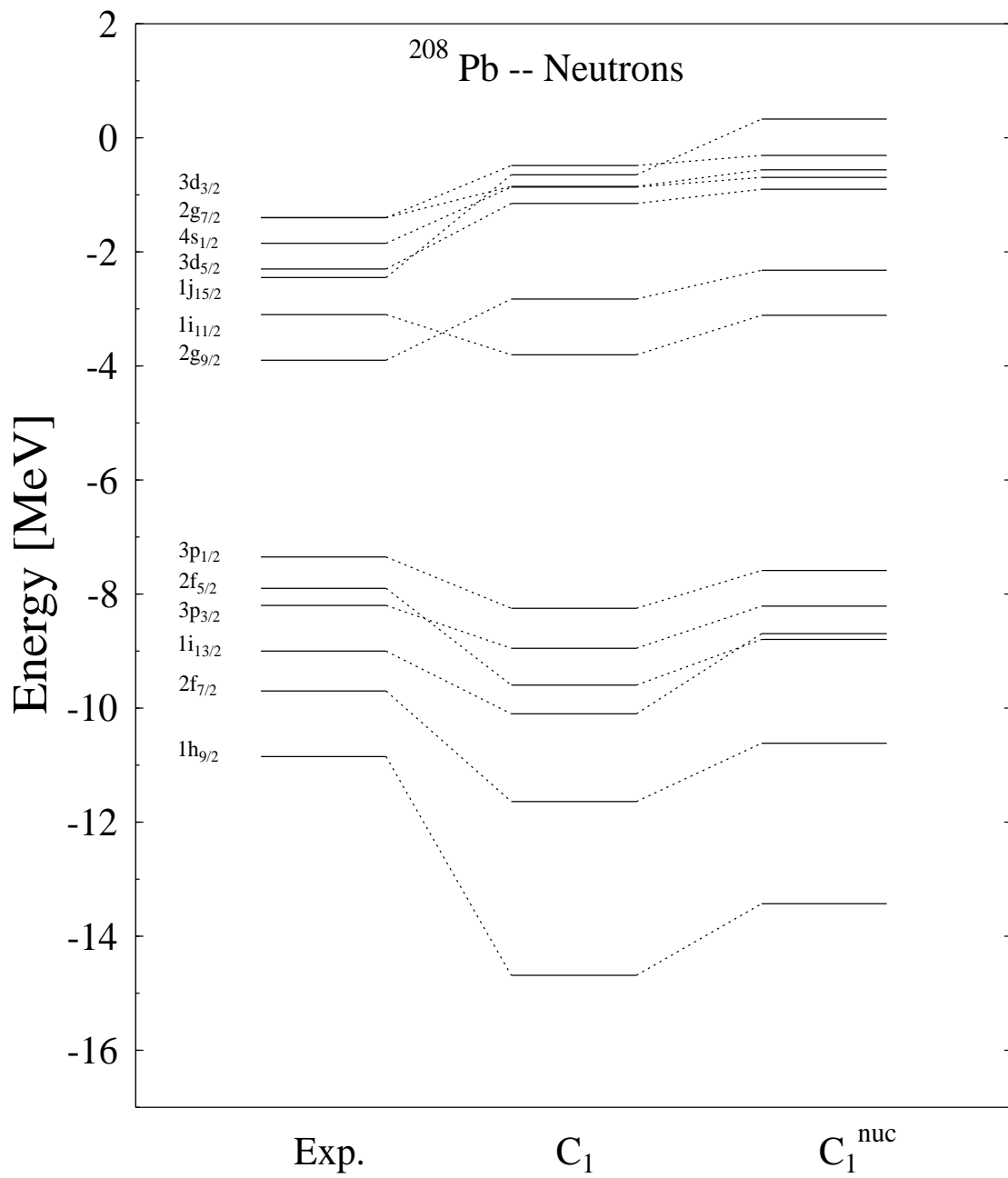


FIG. 4. Single Particle Energies of Neutrons in  $^{208}\text{Pb}$ .

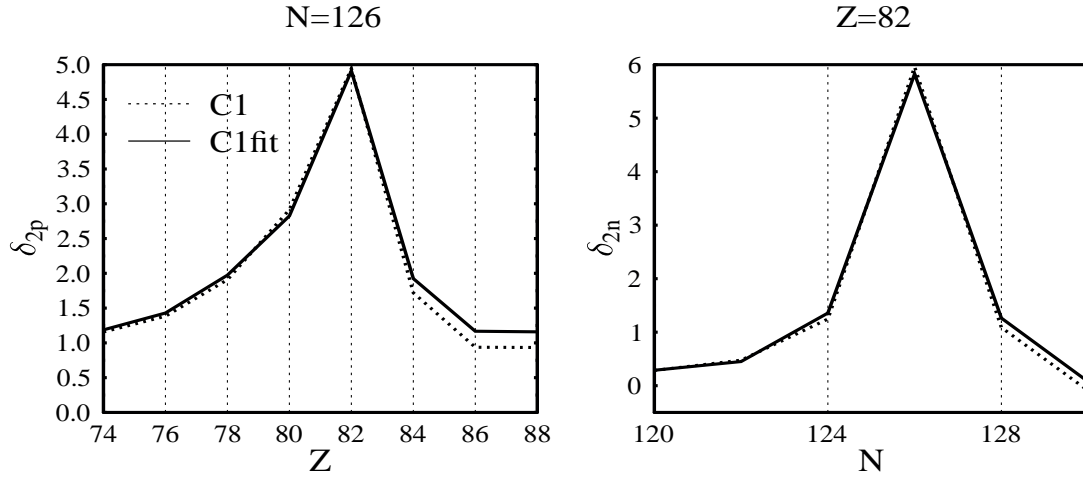


FIG. 5. Two Nucleon Gap-Energy (in MeV) in  $^{208}\text{Pb}$  for Protons and Neutrons.

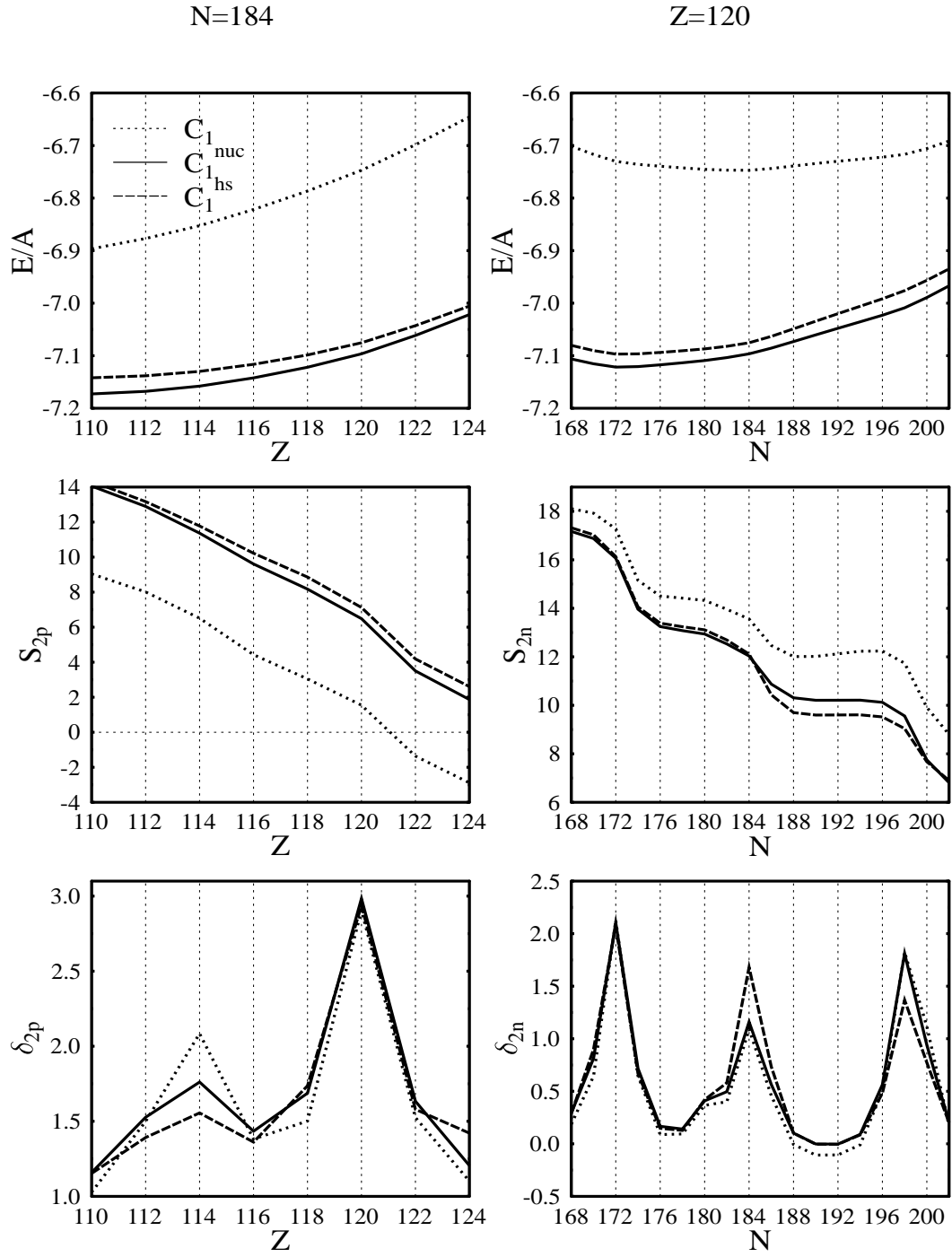


FIG. 6. Binding energy, two nucleon separation energy and two nucleon gap energy for nuclei with 184 neutrons and 120 protons (in MeV).

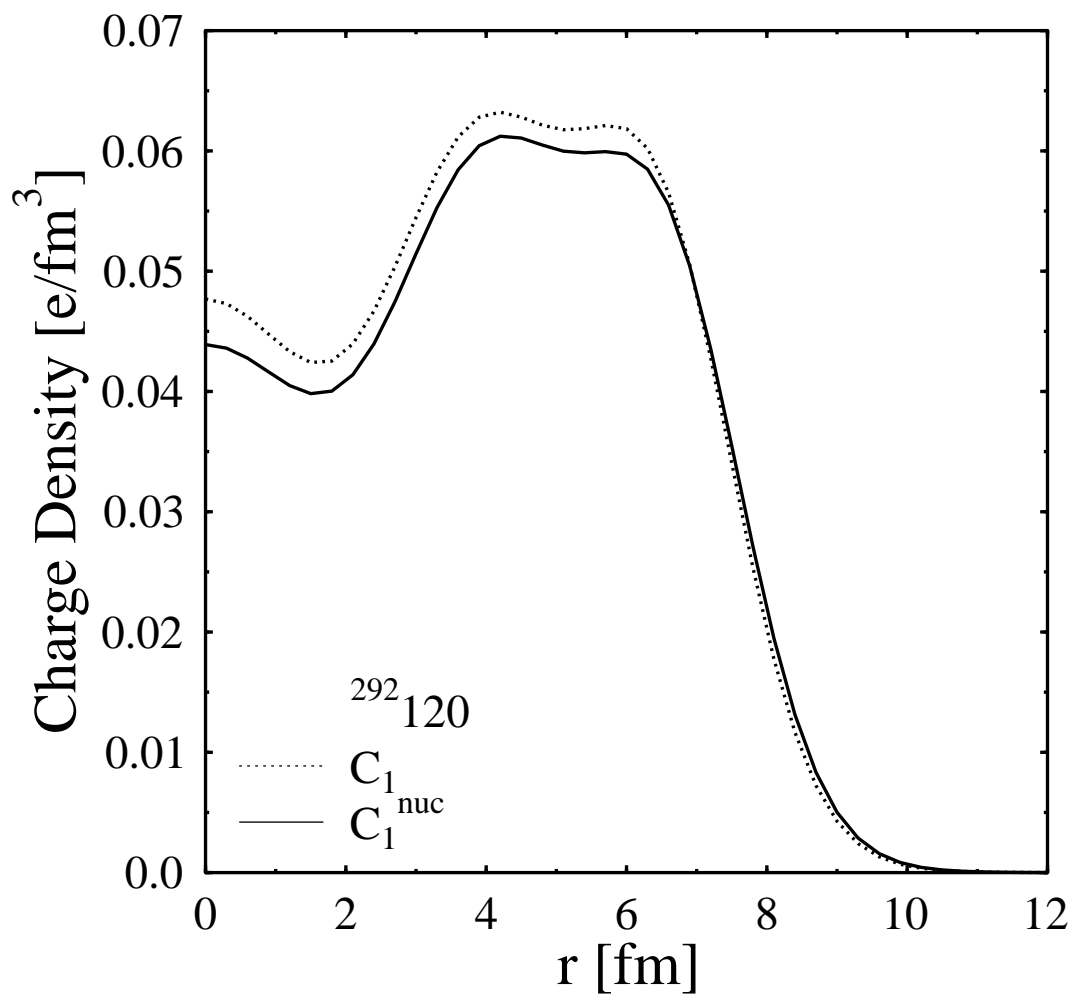


FIG. 7. Charge distribution in the nucleus <sup>292</sup><sub>172</sub>120.

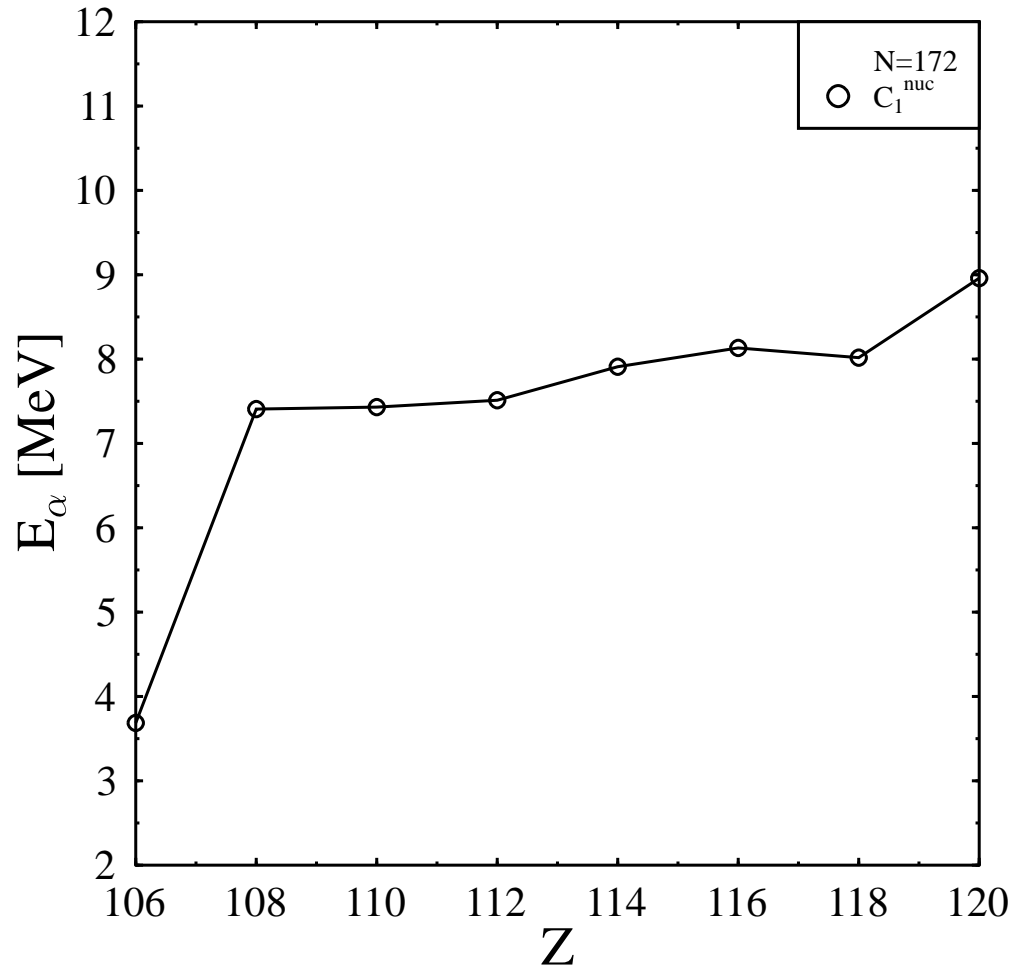


FIG. 8. Energies of the  $\alpha$ -particles emitted in the decay of the nucleus  $^{292}_{120}$ .



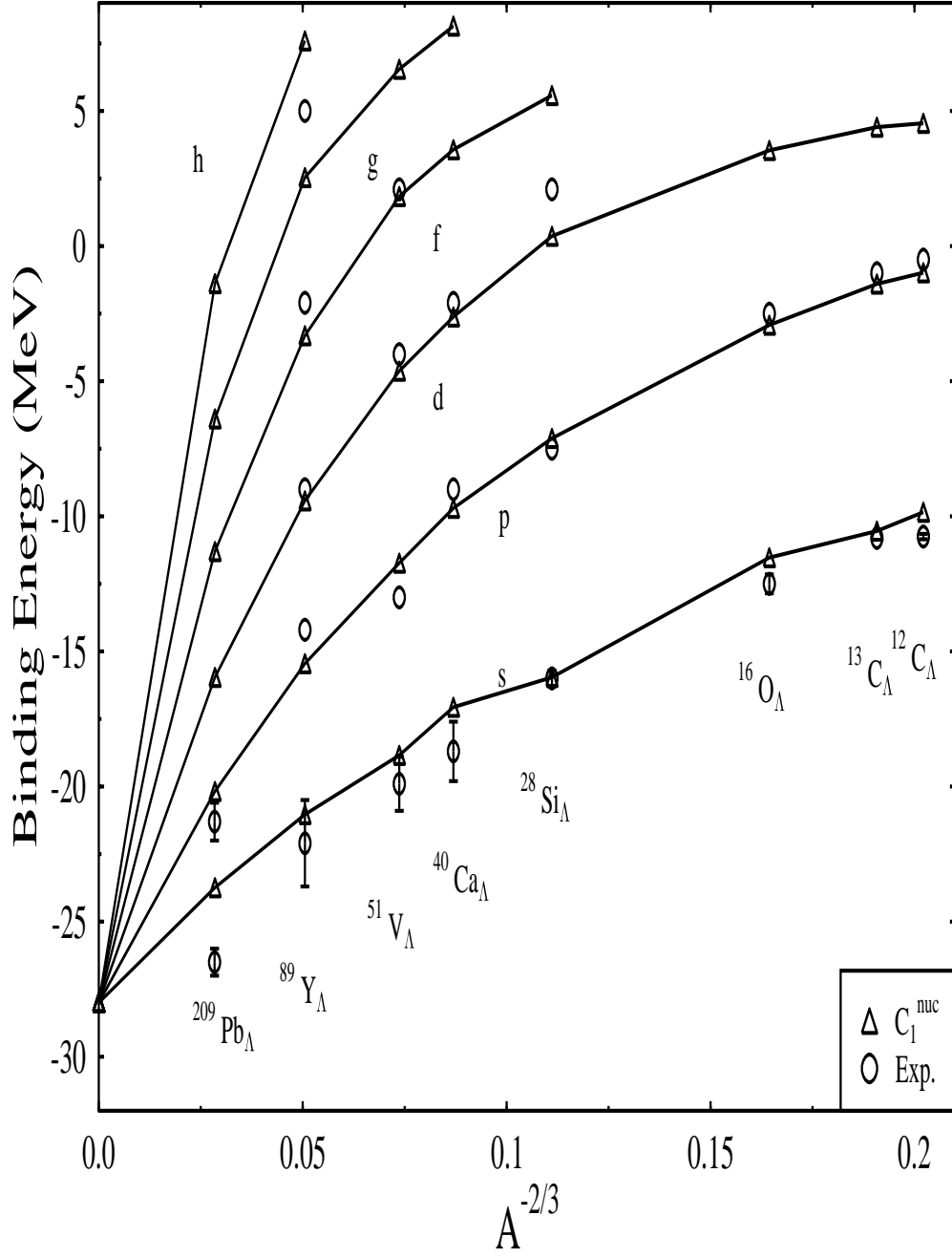


FIG. 9. Single-particle energies of  $\Lambda$ -particles in different nuclei.

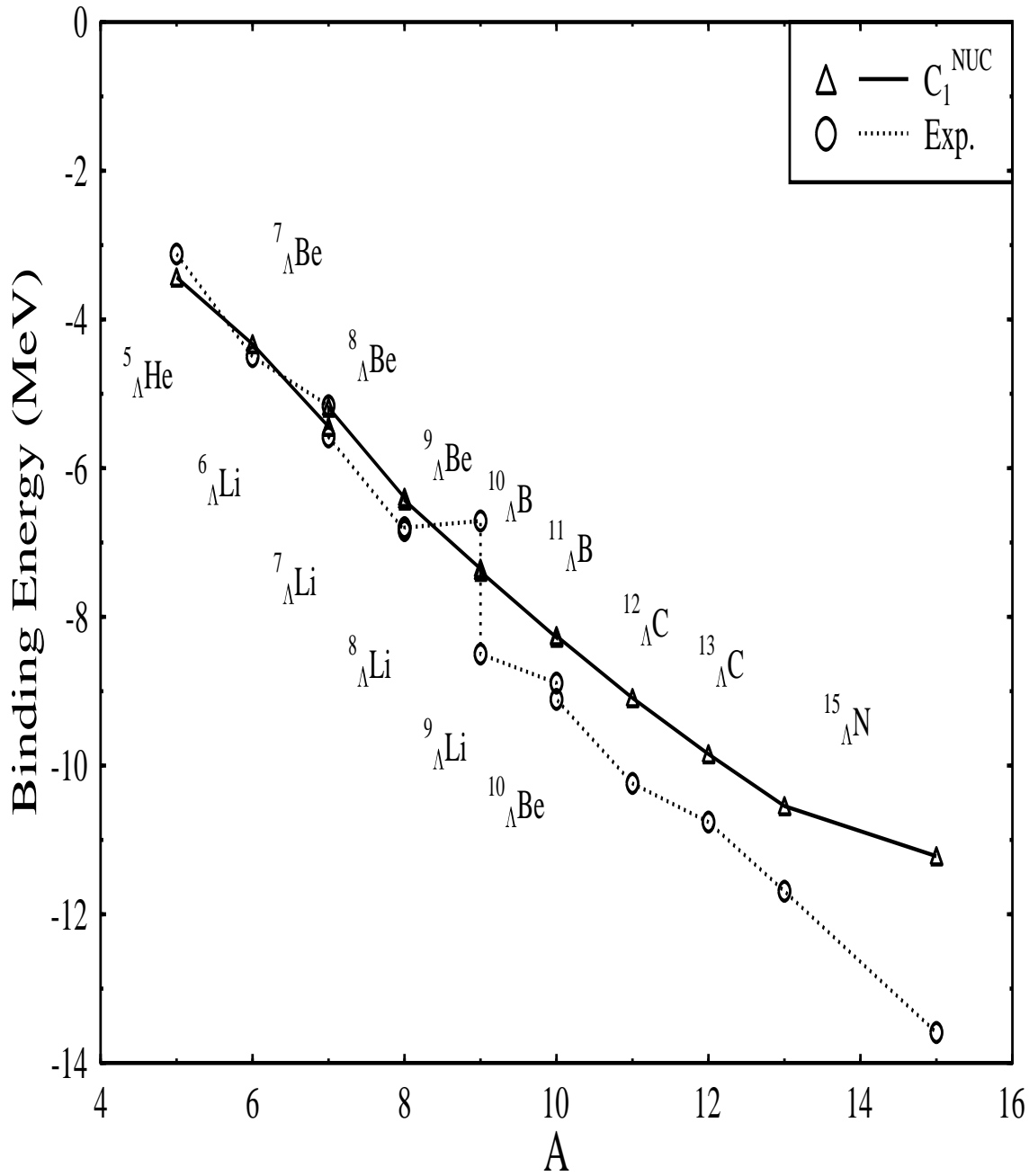


FIG. 10. Binding Energy of  $\Lambda$ -baryons in light nuclei.

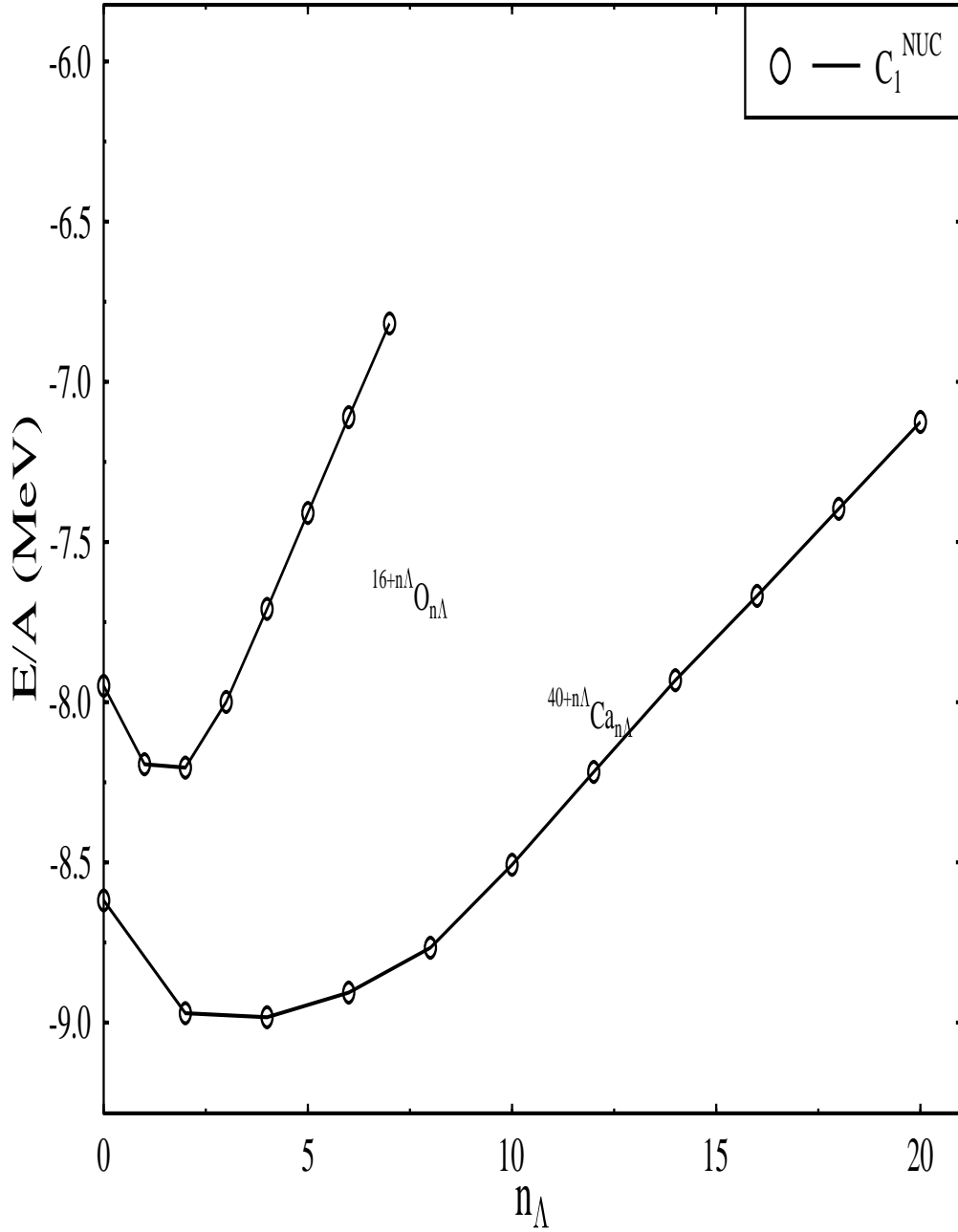


FIG. 11. Binding Energy of nuclei with different numbers of added hyperons.